

Chapter 3

Nonlinear Analysis

3.1 Introduction

Nonlinear analysis investigate the dynamics of observed time-ordered data. Methods of nonlinear analysis, for this thesis, entail determination of embedding parameters, state space reconstruction, uniform time-delay embedding, recurrence plots and recurrence quantification analysis.

The method of state space reconstruction was originally proposed by Packard et al. (1980) and formalised by Takens (1981). Since then, various investigations and disciplines relative to nonlinear time series analysis have benefited from it (Aguirre and Letellier, 2009; Frank et al., 2010; Samà et al., 2013; Stergiou and Decker, 2011). The method of reconstructed state space (RSS) is based on uniform time-delay embedding (UTDE) which is a simple matrix implementation considering the embedding parameters (m and τ), therefore, matrix represents the reconstruction of an unknown d -dimensional manifold M from a scalar time series (e.g. one-dimensional time series in \mathbb{R}). A manifold, in this context, is a multidimensional curved surface within a space (e.g. a saddle) (Guastello and Gregson, 2011). Henceforth, the method of state space reconstruction using a scalar time series can preserve dynamic invariants such as correlation dimension,

fractal dimension, Lyaponov exponents or Kolmogorov-Sinai entropy (Bradley and Kantz, 2015; Krakovská et al., 2015; Quintana-Duque and Saupe, 2013; Quintana-Duque, 2012, 2016). However, there are still many challenging research questions to be answered with regards to the selection of appropriate embedding parameters that preserver the dynamics of a system for the computation of methods nonlinear analysis such as RSS, RPs and RQAs. With that in mind, the following methods are described in this chapter: the state space reconstruction theorem (RSSs), uniform time-delay embedding theorem (UTDE), and methods to compute embedding parameters: false nearest neighbours (FNN) and average mutual information (AMI). Additionally, fundamentals of Recurrence plots(RPs), Recurrence quantification analysis (RQA) and the introduction of 3D surface plots of RQA are presented in this chapter.

3.2 State Space Reconstruction Theorem

Following the notation employed in Casdagli et al. (1991); Garland et al. (2016); Gibson et al. (1992); Takens (1981); Uzal et al. (2011); Uzal and Verdes (2010), the method of state space reconstruction is defined by:

$$s(t) = f^t[s(0)], \quad (3.1)$$

where $s, s : A \rightarrow M$ given that $A \subseteq \mathbb{R}$ and $M \subseteq \mathbb{R}^d$, represents a trajectory which evolves in an unknown d -dimensional manifold M , $f : M \rightarrow M$ is an evolution function and f^t , with time evolution $t \in \mathbb{N}$, is the t -th iteration of f that corresponds to an initial position $s(0) \in M$ (Takens, 1981). Then, a point of a scalar time series $x(t)$ in \mathbb{R} , can be obtained with

$$x(t) = h[s(t)], \quad (3.2)$$

3.3 Uniform Time-Delay Embedding (UTDE)

where h is a function, $h : M \rightarrow \mathbb{R}$, defined on the trajectory $s(t)$.

Reconstructed state space can then be described as an n -dimensional state space defined by $y(t) = \Psi[\mathbf{X}(t)]$ where $\mathbf{X}(t) = \{x(t), x(t - \tau), \dots, x(t - (m - 1)\tau)\}$ is the uniform time-delay embedding with a dimension embedding m and delay embedding τ and $\Psi : \mathbb{R}^m \rightarrow \mathbb{R}^n$ is a further transformation of dimensionality (e.g. Principal Component Analysis, Singular Value Decomposition, etc) being $n \leq m$. With that in mind, uniform time-delay embedding, $\mathbf{X}(t)$, defines a map $\Phi : M \rightarrow \mathbb{R}^m$ such that $\mathbf{X}(t) = \Phi(s(t))$, where Φ is a diffeomorphic map (Takens, 1981) whenever $\tau > 0$ and $m > 2d_{box}$ and d_{box} is the box-counting dimension of M (Garland et al., 2016). Then, if Φ is an embedding of an attractor (i.e. evolving trajectories) in the reconstructed state space, a composition of functions represented with F^t is induced on the reconstructed state space:

$$\mathbf{X}(t) = F^t[\mathbf{X}(0)] = \Phi \circ f^t \circ \Phi^{-1}[\mathbf{X}(0)]. \quad (3.3)$$

Hence, an embedding is defined as "a smooth one-to-one coordinate transformation with a smooth inverse" (Casdagli et al., 1991, p. 54). Figure 3.1 illustrates the state space reconstruction.

3.3 Uniform Time-Delay Embedding (UTDE)

Frank et al. (2010) and Samà et al. (2013) refer to the state space reconstruction outlined in 3.2 as "time-delay embeddings" or "delay coordinates", respectively. However, the term "uniform time-delay embedding" is considered as being more descriptive and appropriate terminology for this thesis.

The uniform time-delay embedding is represented as a matrix of uniform delayed copies of the time series $\{\mathbf{x}_n\}_{n=1}^N$ where N is the sample length of $\{\mathbf{x}_n\}$ and n is index for the samples of $\{\mathbf{x}_n\}$. $\{\mathbf{x}_n\}_{n=1}^N$ has a sample rate of T . The delayed copies

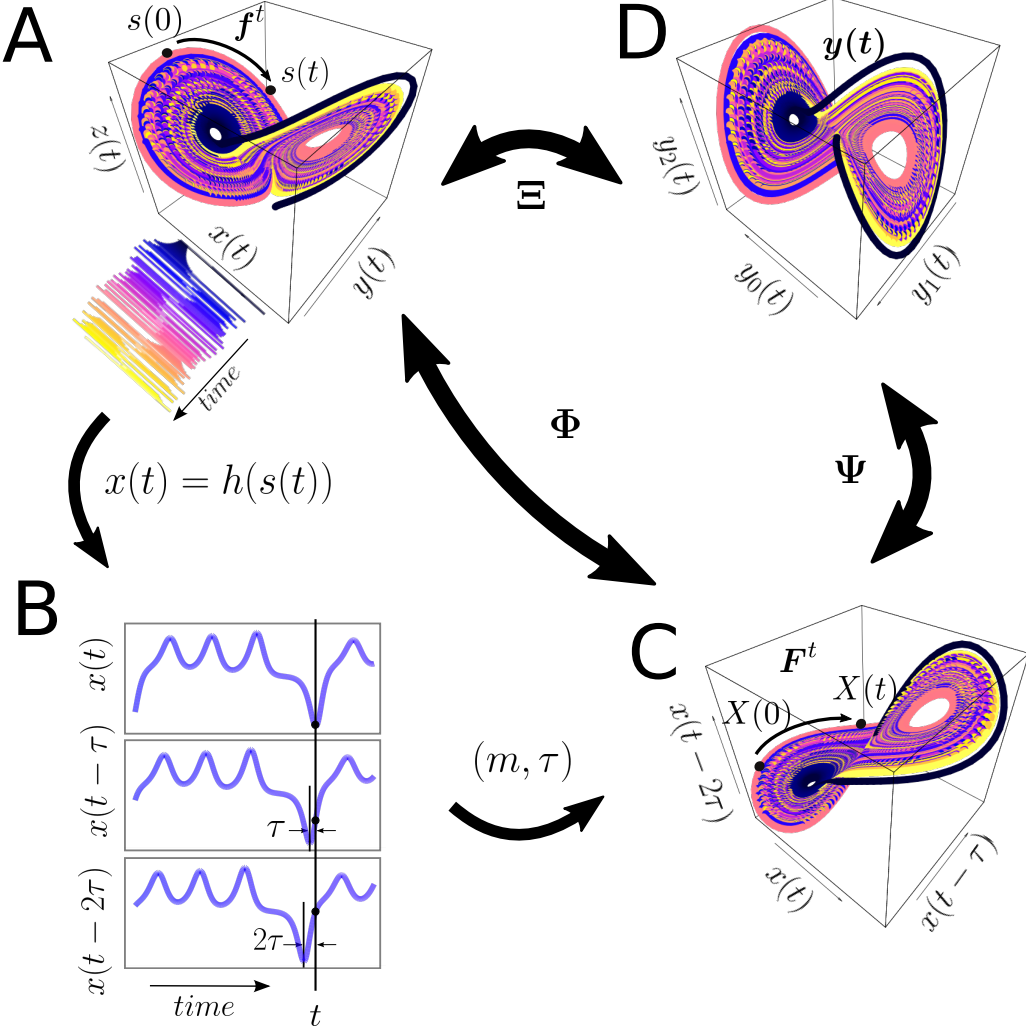


Fig. 3.1 State space reconstruction methodology. State space reconstruction is based on $x(t) = h[s(t)] = h[f^t[s(0)]]$ where $h[]$ is a function $h : M \rightarrow \mathbb{R}$, defined on the trajectory $s(t)$. f is the true dynamical system, $f : M \rightarrow M$, defined as evolution function and f^t , with time evolution $t \in \mathbb{N}$ which is the t -th iteration of f that corresponds to an initial position $s(0) \in M$. The time-delay embedding represented as Φ , maps the original d -dimensional state $s(t)$ into the m -dimensional uniform time-delay embedding matrix $\mathbf{X}(t)$. The transformation map Ψ maps $\mathbf{X}(t)$ into a new state space $y(t)$ of dimensions $n < m$. (A) M -dimensional state space (e.g. Lorenz system); (B) Delayed copies of 1-dimensional $x(t)$ from the Lorenz system; (C) m -dimensional reconstructed state space with m and τ , and (D) $y(t)$ is the n -dimensional reconstructed state space. The total reconstruction map is represented as $\Xi = \Psi \circ \Phi$ where Φ is the delay reconstruction map and Ψ is the coordinate transformation map. This figure is adapted from the work of Casdagli et al. (1991); Quintana-Duque (2012); Uzal et al. (2011). R code to reproduce the figure is available at [\[link\]](#).

3.4 Estimation of Embedding Parameters

of $\{\mathbf{x}_n\}$ are uniformly separated by τ and represented as $\{\tilde{\mathbf{x}}_{n-i\tau}\}$ where i goes from $0, 1, \dots, (m - 1)$ (Fig 3.2). $\{\tilde{\mathbf{x}}_{n-i\tau}\}$ contains information of unobserved state variables and encapsulates the information of the delayed copies of the available time series in the uniform time-delay embedding matrix \mathbf{X}_τ^m , $\mathbf{X}_\tau^m \in \mathbb{R}^m$, defined as

$$\mathbf{X}_\tau^m = \begin{pmatrix} \tilde{\mathbf{x}}_n \\ \tilde{\mathbf{x}}_{n-\tau} \\ \tilde{\mathbf{x}}_{n-2\tau} \\ \vdots \\ \tilde{\mathbf{x}}_{n-(m-1)\tau} \end{pmatrix}^\top, \quad (3.4)$$

where m is the embedding dimension, τ is the embedding delay and $^\top$ denotes the transpose. m and τ are known as embedding parameters. The matrix dimension of \mathbf{X}_τ^m is defined by $N - (m - 1)\tau$ rows and m columns and $N - (m - 1)\tau$ defines the length of each delayed copy of $\{\tilde{\mathbf{x}}_n\}$ in \mathbf{X}_τ^m . A graphical representation of uniform time-delay embedding is shown in Figure 3.2. See Appendix A for further details and explicit examples of uniform time-delay embedding methodology.

3.4 Estimation of Embedding Parameters

The estimation of the embedding parameters (m and τ) is an essential step for the state space reconstruction in order to apply the method of uniform time-delay embedding (UTDE). Hence, two of the most common algorithms are reviewed, which will be used in this thesis, to compute the embedding parameters: the false nearest neighbour (FNN) and the average mutual information (AMI).

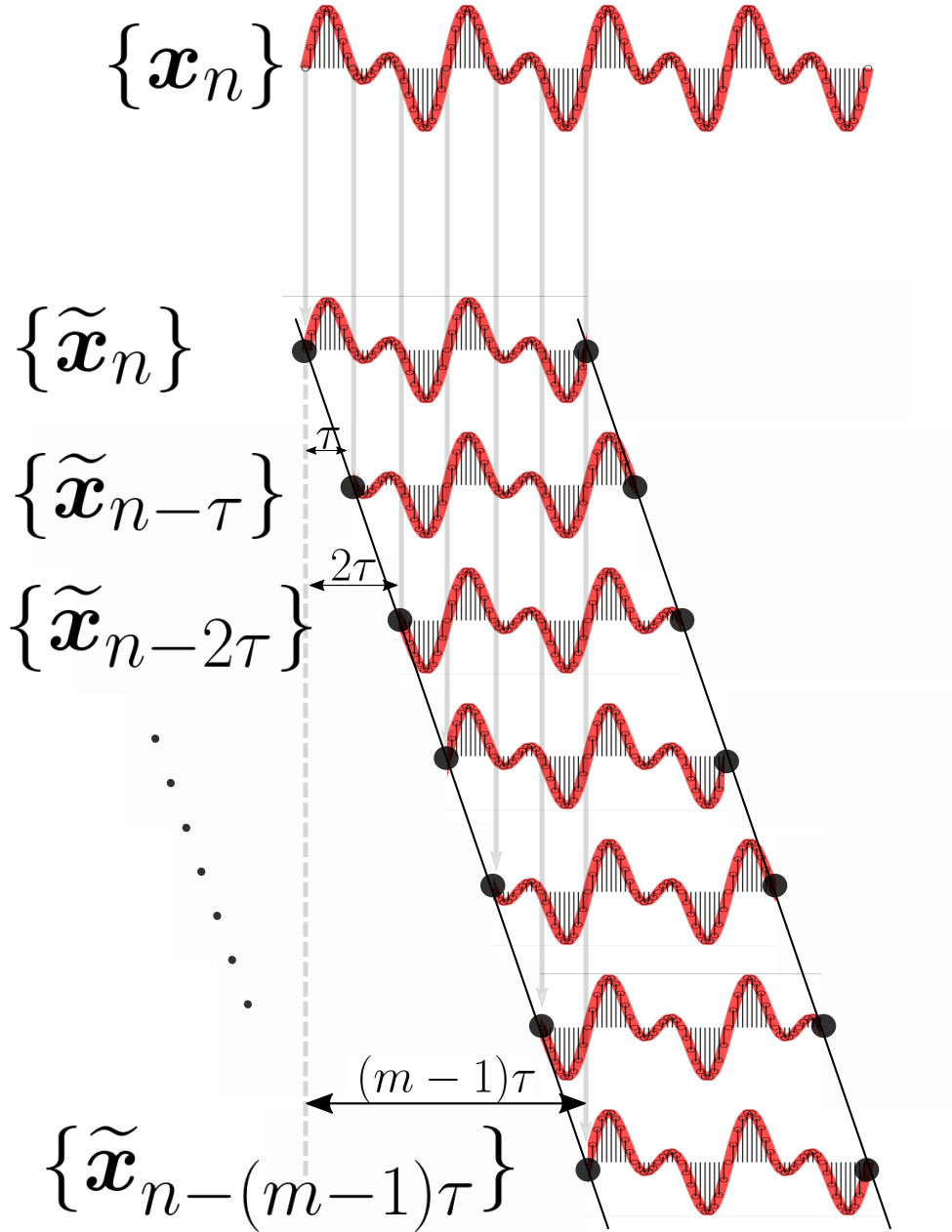


Fig. 3.2 **Uniform time-delay embedding (UTDE).** UTDE is illustrated as $m - 1$ delayed copies of $\{x_n\}$ which is uniformly separated by τ . UTDE is represented as $\{\tilde{x}_n, \dots, \tilde{x}_{n-(m-1)\tau}\}$ (Eq. 3.4). R code to reproduce the figure is available at [🔗](#).

3.4.1 False Nearest Neighbours (FNN)

To select the minimum embedding dimension m_0 , Kennel et al. (1992) used the method of false neighbours which can be understood as follows: on one hand, when the embedding dimension is too small to unfold the attractor (i.e. evolving trajectories in a state space) "not all points that lie close to each other will be neighbours and some points appear as neighbours as a result of the attractor being projected down into a smaller space", on the other hand, when increasing the embedding dimension "points that are near to each other in the sufficient embedding dimension should remain close as the dimension increase from m to $m + 1$ " (Krakovská et al., 2015, p. 3).

From a mathematical point of view, state space reconstruction is done when the attractor is unfolded with either the minimum embedding dimension, m_0 , or any other embedding dimension value where $m \geq m_0$ (Kennel et al., 1992). In contrast, any large value of m_0 leads to excessive computations (Bradley and Kantz, 2015). Hence, Cao (1997) proposed an algorithm based on the false neighbour method where only the time-series and one delay embedding value are necessary to select the minimum embedding dimension. Cao's algorithm is based on $E(m)$, which is the mean value of all $a(i, m)$, and defined as:

$$\begin{aligned} E(m) &= \frac{1}{N - m\tau} \sum_{i=1}^{N-m\tau} a(i, m) \\ &= \frac{1}{N - m\tau} \sum_{i=1}^{N-m\tau} \frac{\|\mathbf{X}_i(m+1) - \mathbf{X}_{n(i,m)}(m+1)\|}{\|\mathbf{X}_i(m) - \mathbf{X}_{n(i,m)}(m)\|} \end{aligned} \quad (3.5)$$

where $\mathbf{X}_i(m)$ and $\mathbf{X}_{n(i,m)}(m)$ are uniform time-delay embeddings with $i = 1, 2, \dots, N - (m - 1)\tau$ and $n(i, m) = 1 \leq n(i, m) \leq N - m\tau$. From Eq. 3.5 $E(m)$ is only dependent on m and τ for which $E_1(m)$ is defined as

$$E_1(m) = \frac{E(m+1)}{E(m)}. \quad (3.6)$$

Nonlinear Analysis

$E_1(m)$ is therefore proposed to describe the variation from m to $m + 1$ in order to find the minimum embedding dimension m_0 (Eq. 3.6). As Cao 1997, p. 44 described: " $E_1(m)$ stops changing when m is greater than some m_0 , if the time series comes from a multidimensional state space then $m_0 + 1$ is the minimum dimension". Additionally, Cao (1997) proposed $E_2(m)$ to distinguish deterministic signals from stochastic signals.

$E_2(m)$ is defined as

$$E_2(m) = \frac{E^*(m+1)}{E^*(m)}, \quad (3.7)$$

where

$$E^*(m) = \frac{1}{N - m\tau} \sum_{i=1}^{N-m\tau} \|\mathbf{X}_i(m+1) - \mathbf{X}_{n(i,m)}(m+1)\|. \quad (3.8)$$

For instance, when the signal comes from random noise (values that are independent from each other), all $E_2(m)$ values are approximately equal to 1 (e.g. $E_2(m) \approx 1$). However, for deterministic data $E_2(m)$ is not constant for all m (e.g. $E_2(m) \neq 1$).

Two time series are considered as an example of the use of $E_1(m)$ and $E_2(m)$ values, the solution for the x variable of the chaotic deterministic Lorenz system (Figure 3.3E), and a Gaussian noise time series with zero mean and a variance of one (Figure 3.3F). Then $E_1(m)$ and $E_2(m)$ values are computed for each time series. The $E_1(m)$ values for the chaotic time series appear to be constant after the dimension is equal to six. The determination of six is given that any value of m can be used as $E_1(m)$ values are within the threshold of 1 ± 0.05 (Fig 3.3A). Although the $E_2(m)$ values for the chaotic time series tend to be closer to one as m increases, these are different to one (Fig 3.3C), for which, it can be concluded that the chaotic time series comes from a chaotic deterministic signal. With regard to the noise time series, $E_1(m)$ values appeared to be constant when m is close to thirteen which is defined by the same threshold of 1 ± 0.05 (Figure 3.3B). Then, contrary to the $E_2(m)$ values for a chaotic Lorenz time series, all values of $E_2(m)$ for a noise time series are approximately equal to one (Figure 3.3D). Hence, $E_1(m)$ values then indicate the minimum embedding

3.4 Estimation of Embedding Parameters

dimension of the noisy time series is thirteen, however all of the $E_2(m)$ values are approximately equal to one (Figure 3.3D), for which, it can be concluded that noise time series is a stochastic signal.

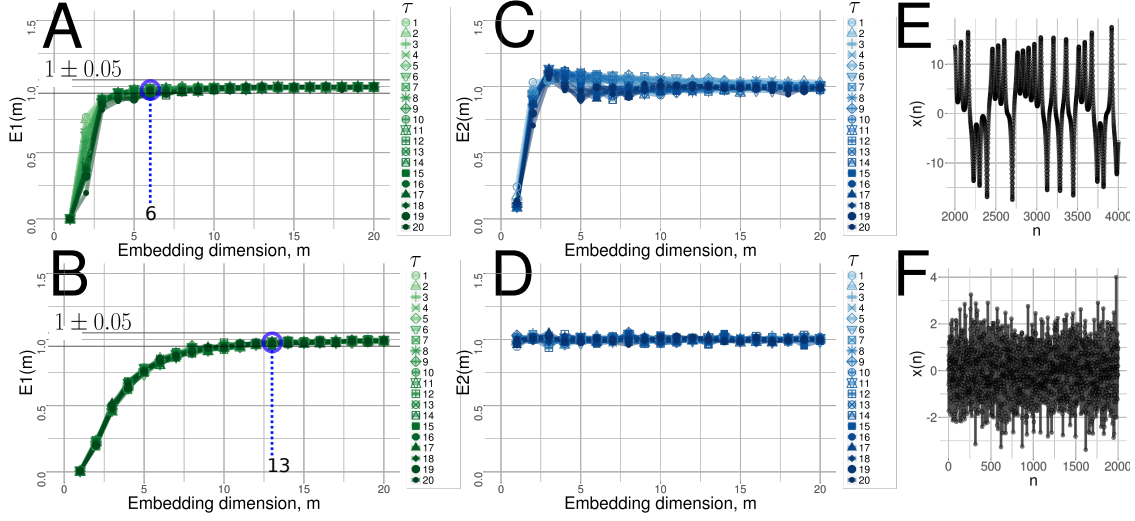


Fig. 3.3 Minimum dimension embedding values with Cao’s method. (A, B) $E_1(m)$ values and (C, D) $E_2(m)$ values with variations of τ values from one to twenty for (E) chaotic and (F) random time series. R code to reproduce the figure is available at [\[4\]](#).

It is important to note that for this thesis not only the values for $E_1(m)$ and $E_2(m)$ are computed but also a variation of τ from 1 to 20 (Figure 3.3 (A,B,C,D)) has been explored. The purpose of using variations for τ is to show its independence with regard to the $E_1(m)$ (Fig. 3.3(A,B)) and $E_2(m)$ (Fig. 3.3(C,D)). Although Cao (1997) mentioned that no parameters are required to find the minimum embedding dimension, it has been found, in this thesis, that it is necessary to define a threshold for which $E_1(m)$ values appear to be constant. Hence, for the given examples and the reported results for this thesis, a threshold of 0.05 is defined (see Fig. 3.3(A) with the parallel lines of the threshold near to one 1 ± 0.05). Additionally, see optimal embedding parameters on Chapter 7 for further research regarding the selection of such threshold.

3.4.2 Average Mutual Information (AMI)

One would experience the following when selecting the delay dimension parameter, τ :

- (i) when τ is too small, the elements of uniform time-delay embedding will be along the bisectrix of the phase space and the reconstruction is generally not satisfactory,
- (ii) when τ is too large the elements of the uniform time-delay embedding will become spread and uncorrelated which makes recovering the underlying attractor (i.e. evolving trajectories in a state space) difficult, if not impossible (Casdagli et al., 1991; Emrani et al., 2014; Garcia and Almeida, 2005).

There are many approaches to compute the embedding parameters (Bradley and Kantz, 2015), for instance, geometry-based methodologies where the amount of space filled in the reconstructed state is the metric to compute the delay embedding (Rosenstein et al., 1994) or theoretical approaches to estimate an optimal parameter for τ (Casdagli et al., 1991). However, the autocorrelation function and the average mutual information (AMI) are the two most commonly used algorithms to compute the minimum delay embedding parameter τ_0 . Emrani et al. (2014) used the autocorrelation function in which the first zero crossing is considered as the minimum delay embedding parameter. However, the autocorrelation function is a linear statistic whereas AMI considers the nonlinear dynamical correlations (Fraser and Swinney, 1986; Krakovská et al., 2015). With that in mind, the AMI algorithm is described below to estimate the minimum delay embedding parameter, τ_0 .

To compute the AMI, an histogram of $x(n)$ using n bins is calculated and then a probability distribution of data is computed (Kantz and Schreiber, 2003). AMI is therefore denoted by $I(\tau)$ which is the average mutual information between the original time series, $x(n)$, and the delayed time series, $x(n - \tau)$, delayed by τ (Kabiraj et al., 2012). AMI is defined by

$$I(\tau) = \sum_{i,j}^N p_{ij} \log_2 \frac{p_{ij}}{p_i p_j}, \quad (3.9)$$

3.4 Estimation of Embedding Parameters

where probabilities are defined as follows: p_i is the probability that $x(n)$ has a value inside the i -th bin of the histogram, p_j is the probability that $x(n+\tau)$ has a value inside the j -th bin of the histogram and $p_{ij}(\tau)$ is the probability that $x(n)$ is in bin i and $x(n+\tau)$ is in bin j . The AMI is measured in bits (base 2, also called shannons) (Garcia and Sawitzki, 2016; Kantz and Schreiber, 2003). For small τ ($\tau < 3$), AMI will be large ($I(\tau) > 6$) and as m increase AMI will then decrease rapidly. Hence, as τ increase and goes to a large limit, $x(n)$ and $x(n+\tau)$ have nothing to do with each other and p_{ij} is factorised as $p_i p_j$ for which AMI is close to zero. Then, in order to obtain τ_0 , "it has to be found in the first minimum of $I(\tau)$ where $x(n+\tau)$ adds maximal information to the knowledge from $x(n)$ " meaning that the redundancy between $x(n+\tau)$ and $x(n)$ is the least (Kantz and Schreiber, 2003, p. 151).

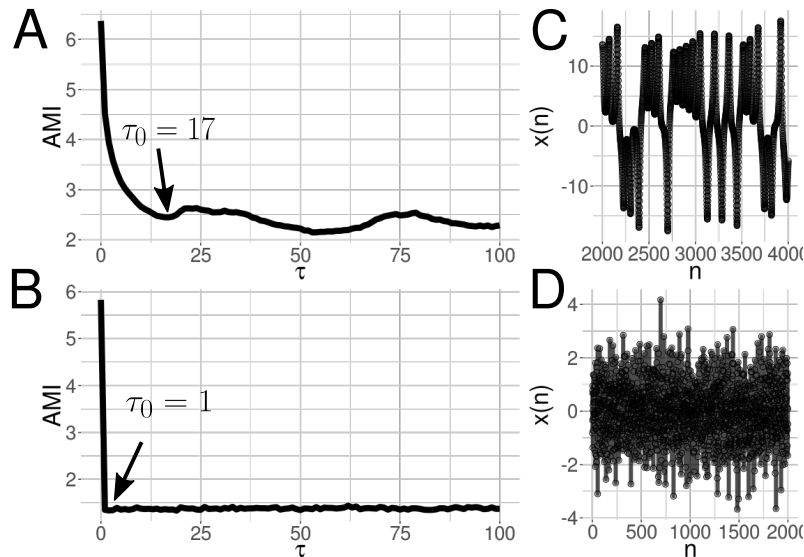


Fig. 3.4 Minimum delay embedding values with AMI's method. (A, B) AMI values where its first minimum value in the curve is the minimum time delay embedding (τ_0), for (C) a chaotic and (D) noise time series. R code to reproduce the figure is available at [\[link\]](#).

For example, the AMI is computed for two time series: (i) the x solution of the deterministic chaotic Lorenz system, and (ii) a noise time series using a normal distribution with mean zero and standard deviation equal to one. The AMI plots are

shown in Figure 3.4, where the minimum delay embedding parameter for the chaotic time series is $\tau_0 = 17$ and for the noise time series is $\tau_0 = 1$. Hence, it can be concluded that the amount of knowledge for any noise time series is zero for which the first minimum embedding parameter is equal to one. On the contrary, the first minimum of the AMI for the chaotic time series is $\tau_0 = 17$ which is the value that maximize the independence in the reconstructed state space (Bradley and Kantz, 2015).

3.4.3 Overall minimum embedding parameters

The method to select minimum embedding parameters (m_0 and τ_0) for this thesis is firstly to compute m_0 with FNN algorithm (considering a threshold of 0.05 for $E_1(m)$ values) and secondly to compute τ_0 with AMI (which does not need any extra parameter). From the previous example of the deterministic-chaotic Lorenz system, Fig 3.3(A) is used to determine the minimum dimension embedding ($m_0 = 6$) and Fig 3.4(A) is used to determine the minimum delay embedding ($\tau_0 = 17$). Therefore, with the computation of the minimum embedding parameters, the reconstructed attractor is created in order to ensure with τ_0 the maximum independence between $x(t)$ and $x(t + \tau_0)$ and with m_0 allowing the trajectories in the reconstructed state space to be unfolded.

As time-series data for this thesis are multidimensional (i.e. more than one time series), sample mean of individual minimum values m_{0_i} and τ_{0_i} is used to get an overall value of embedding minimum embedding parameters \bar{m}_0 and $\bar{\tau}_0$ (Eqs. 3.10 and 3.11):

$$\bar{m}_0 = \frac{1}{N} \sum_{i=1}^N m_{0_i}, \quad (3.10)$$

and

$$\bar{\tau}_0 = \frac{1}{N} \sum_{i=1}^N \tau_{0_i}, \quad (3.11)$$

where N is the number of time series and $i = 1, \dots, N$.

It is also important to mention that a maximum of individual minimum dimension embeddings, m_{0i} , can be used instead of the overall sample mean of individual minimum dimension embeddings. The rationale for that is because the maximum value can unfold trajectories in the reconstructed state space that require a lower embedding dimension value. However such statement might be different for the maximum of individual minimum embedding delay as such maximum might not create the maximum independence between $x(n)$ and $x(n + \tau)$ for multiple time-series data. See Chapter 7 for future research on optimal embedding parameters.

3.5 Reconstructed State Space with UTDE

Given a time series $x(n)$, the UTDE matrix is computed with its minimum embedding parameters and then Principal Component Analysis (PCA) is applied in order to select the first three axis of the rotated data to create the reconstructed state spaces (Frank et al., 2010; Samà et al., 2013). See Fig. 3.1 that illustrates and describes the method of reconstructed state space with UTDE.

3.6 Recurrence Plots (RP)

Henri Poincaré in 1890 introduced the concept of recurrences in conservative systems, however the discovery was not put into practice until the development of faster computers (Marwan et al., 2007), for which Eckmann et al. (1987) introduced a method where recurrences in the dynamics of a system can be visualised. The intention of Eckmann et al. (1987) was to propose a tool, called Recurrence Plot (RP), that provides insights into high-dimensional dynamical systems where trajectories are very difficult to visualise. Hence, "RP is a tool that helps us to investigate the m -dimensional phase

Nonlinear Analysis

space trajectories through a two-dimensional representation of its recurrences" (Marwan and Webber, 2015, p. 7). Similarly, Marwan and Webber (2015) pointed out that in addition to the methodologies of the state space reconstruction and other dynamic invariants (e.g. Lyapunov exponent, Kolmogorov-Sinai entropy), the recurrences of the trajectories in the phase space can provide important clues to characterise the underlying process for periodicities (as Milankovitch cycles) or irregular cycles (as El Niño Southern Oscillation). Such recurrences can not only be visualised using Recurrence Plots (RP) but also be quantified with Recurrence Quantification Analysis (RQA) metrics, which leads to applications of these tools in various areas such as Economics, Physiology, Neuroscience, Earth Science, Astrophysics and Engineering (Marwan et al., 2007).

A recurrence plot based on time series $\{\mathbf{x}_n\}$ is computed from the state space reconstruction with uniform time-delay embedding method $X(i) = \{\tilde{\mathbf{x}}_n, \dots, \tilde{\mathbf{x}}_{n-(m-1)\tau}\}$ where $i = 1, \dots, N$, N is the number of considered states of $X(i)$ where $X(i) \in \mathbb{R}^m$ (Eckmann et al., 1987). The recurrence plot is therefore a two-dimensional $N \times N$ square matrix, \mathbf{R} , where a black dot is placed at (i, j) whenever $X(i)$ is sufficiently close to $X(j)$:

$$\mathbf{R}_{i,j}^m(\epsilon) = \Theta(\epsilon_i - \|X(i) - X(j)\|), \quad X(i) \in \mathbb{R}^m, \quad i, j = 1, \dots, N, \quad (3.12)$$

where ϵ is a threshold distance, $\|\cdot\|$ a norm, and $\Theta(\cdot)$ is the Heaviside function (i.e. $\Theta(x) = 0$, if $x < 0$, and $\Theta(x) = 1$ otherwise) (Fig 3.5) (Eckmann et al., 1987; Marwan et al., 2007; Marwan and Webber, 2015). RP is also characterised with a line of identity (LOI) which is a black main diagonal line due to $R_{i,j} = 1$ for $i, j = 1, \dots, N$.

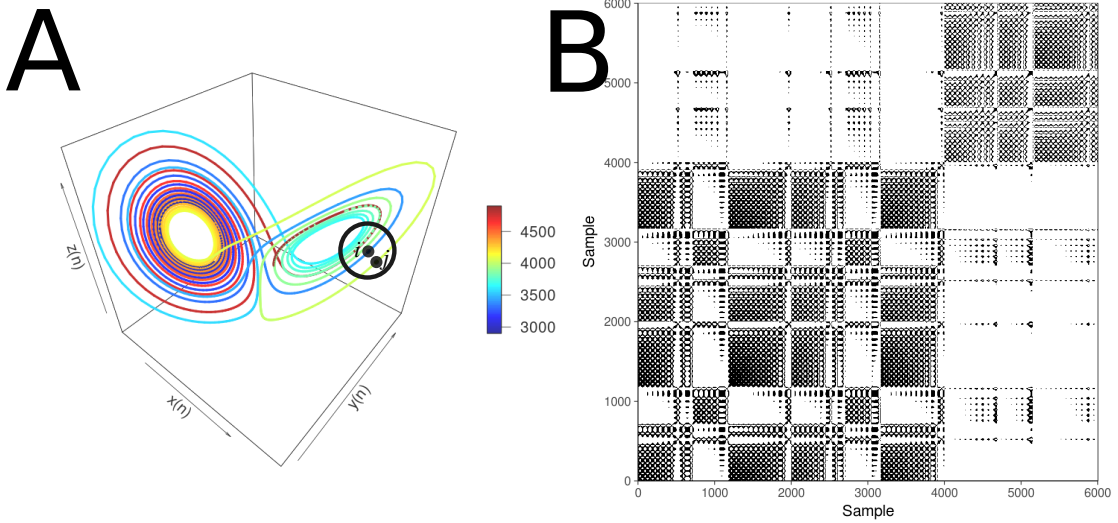


Fig. 3.5 Recurrence Plots. (A) State space of the Lorenz system with controlling parameters ($\rho = 28, \sigma = 10, \beta = 8/3$). A point, j , in trajectory $X()$ which falls into the neighborhood (black circle) of a given point at i is a recurrent point and is represented as a black dot in the recurrence plot at location (i, j) or white otherwise. (B) Recurrence plot using the three components of the Lorenz system and the RP with no embeddings and threshold $\epsilon = 5$. This figure is adapted from Marwan and Webber (2015). R code to reproduce the figure is available at [\[link\]](#).

3.6.1 Structures of Recurrence Plots

Pattern formations in RPs can be designated either as topology for large-scale patterns or texture for small-scale patterns. In the case of topology, the following pattern formations are presented: (i) homogeneous where uniform recurrence points are spread in the RP e.g., uniformly distributed noise (Figure 3.6A), (ii) periodic and quasi-periodic systems where diagonal lines and checkerboard structures represent oscillating systems, e.g., sinusoidal signals (Figure 3.6B), (iii) drift where paling or darkening recurrence points away from the LOI is caused by drifting systems, e.g., logistic map (Figure 3.6C), and (iv) disrupted where recurrence points are presented white areas or bands that indicate abrupt changes in the dynamics, e.g. Brownian motion (Figure 3.6D) (Eckmann et al., 1987; Marwan and Webber, 2015). Texture, for small-

Nonlinear Analysis

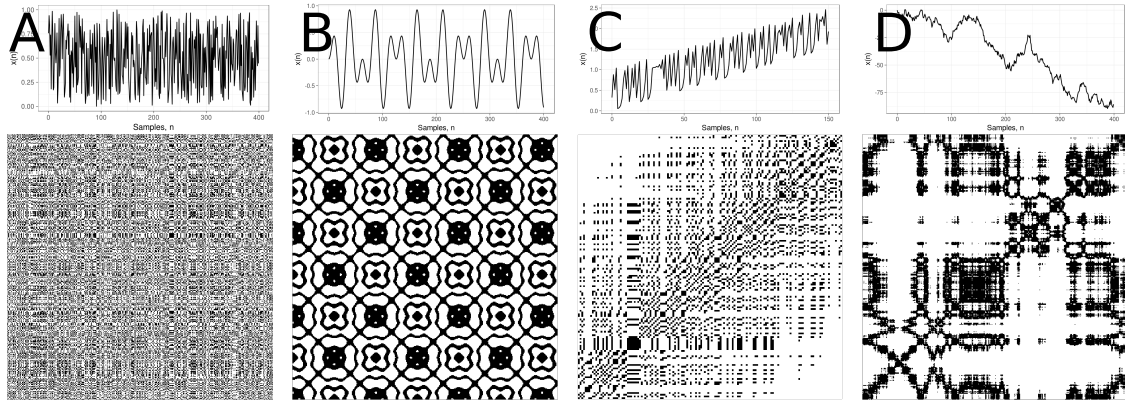


Fig. 3.6 Patterns in Recurrence Plots. Time-series with its respective recurrence plots for: (A) uniformly distributed noise, (B) super-positioned harmonic oscillation ($\sin \frac{1}{5}t \sin \frac{5}{100}t$), (C) drift logistic map ($x_{i+1} = 4x_i(1 - x_i)$) corrupted with a linearly increase term ($0.01i$), and (D) disrupted brownian motion ($x_{i+1} = x_i + 2rnorm(1)$). Figure is adapted from Marwan and Webber (2015). R code to reproduce the figure is available at [🔗](#).

scale patterns, can be categorised as: (i) single or isolated recurrence points that represent rare occurring states, do not persist for any time or fluctuate heavily, (ii) dots forming diagonal lines where the length of the small-scale parallel lines in the diagonal are related to the ratio of determinism or predictability in the dynamics of the system, and (iii) dots forming vertical and horizontal lines where the length of the lines represent a time length where a state does not change or change very slowly and the patterns formation represent discontinuities in the signal, and (iv) dots clustering to inscribe rectangular regions which are related to laminar states or singularities (Marwan and Webber, 2015).

Although, the previous pattern descriptions of the structures in the RP offer an idea of the characteristics of dynamical systems from time-series, these descriptions might be misinterpreted and conclusions might tend to be subjective as these require the interpretation of a researcher(s). Because of that, recurrence quantification analysis (RQA) offers objective metrics to quantify the visual characteristics of recurrent pattern structures in the RP (Zbilut and Webber, 1992).

3.7 Recurrence Quantifications Analysis (RQA)

Zbilut and Webber (1992) proposed metrics to investigate the density of recurrence points in RPs, then histograms of lengths for diagonal lines in RPs were studied by Trulla et al. (1996), then Marwan (2008) introduced the term Recurrence Quantification Analysis (RQA). There are different RQA metrics such as percentage of recurrence, percentage of determinism, ratio, Shannon entropy of the frequency distributions of the line lengths, maximal line length and divergence, trend and laminarity (Marwan et al., 2007; Marwan and Webber, 2015). For this thesis, I therefore considered only four RQA metrics (i.e. REC, DET, RATIO and ENT) due to their relationship with the variables of complexity and predictability from models of movement variability (Stergiou et al., 2006; Vaillancourt and Newell, 2002, 2003).

3.7.1 Measures of RP based on the recurrence density

The percentage of recurrence (REC) or recurrence rate (RR) is defined as

$$REC(\epsilon, N) = \frac{1}{N^2 - N} \sum_{i \neq j=1}^N \mathbf{R}_{i,j}^m(\epsilon), \quad (3.13)$$

which enumerates the black dots in the RP excluding the line of identity. RR is a measure of the relative density of recurrence points in the sparse matrix (Marwan and Webber, 2015).

3.7.2 Measures of RP based on diagonal lines

The percent of determinism (DET) is defined as the fraction of recurrence points that form diagonal lines and it is determined by

$$DET = \frac{\sum_{l=d_{min}}^N l H_D l}{\sum_{i,j=1}^N \mathbf{R}_{i,j}(\epsilon)}, \quad (3.14)$$

Nonlinear Analysis

where

$$H_D(l) = \sum_{i,j=1}^N (1 - \mathbf{R}_{i-1,j-1}(\epsilon))(1 - \mathbf{R}_{i+l,j+l}(\epsilon)) \prod_{k=0}^{l-1} \mathbf{R}_{i+k,j+k}(\epsilon) \quad (3.15)$$

is the histogram of the lengths of the diagonal structures in the RP.

DET can be interpreted as the predictability of the system, for instance, periodic signals have longer diagonal lines, chaotic signals have shorter diagonal lines and absent of diagonal lines results from stochastic signals (Marwan et al., 2007; Marwan and Webber, 2015). Similarly, DET is considered as a measurement for the organisation of points in RPs (Iwanski and Bradley, 1998).

RATIO is defined as the ratio between DET and REC and it is calculated from the frequency distributions of the lengths of the diagonal lines. RATIO is useful to discover dynamic transitions (Marwan and Webber, 2015).

ENT is the Shannon entropy of the frequency distribution of the diagonal line lengths and it is defined as

$$ENT = - \sum_{l=d_{min}}^N p(l) \ln p(l) \quad \text{where} \quad p(l) = \frac{H_D(l)}{\sum_{l=d_{min}}^N H_D(l)}. \quad (3.16)$$

ENT reflects the complexity of the deterministic structure in the system. For instance, for uncorrelated noise or oscillations, the value of ENT is rather small and indicates low complexity of the system, therefore "the higher the ENT is the more complex the dynamics are" (Marwan and Webber, 2015, p. 15).

3.7.3 Some weaknesses and strengths of RP and RQA.

One of the main advantages of the use of RP is its capacity to detect small modulations in frequency or phase that are not detectable when using standard methods e.g. spectral or wavelet analysis (Marwan, 2011). Nonetheless, RP is a very young field in nonlinear analysis and many research remains to be done, for instance, RP can create different

3.7 Recurrence Quantifications Analysis (RQA)

results because of different values for embedding parameters and recurrence thresholds for different size of window length of time-series data (Eckmann et al., 1987; Marwan, 2011). Additionally, the selection of recurrence threshold, ϵ , can depend on the system that is under analysis. For instance, when studying dynamical invariants ϵ is required to be very small, for trajectory reconstruction ϵ is required to have a large threshold or when studying dynamical transition there is little importance about the selection of the threshold (Marwan, 2011). Other criteria for the selection of ϵ is that the recurrence threshold should be five times larger than the standard deviation of the observational noise or the use of diagonal structures within the RP is suggested in order to find the optimal recurrence threshold for (quasi-)periodic process (Marwan, 2011).

Iwanski and Bradley (1998) highlighted the importance of choosing appropriate embedding parameters to compute RQA in order to have a better intuition of the nature of the structure of time-series data. In the same investigation, Iwanski and Bradley (1998) pointed out that RQA metrics are quantitatively and qualitatively independent of embedding dimension. However, with an example, Iwanski and Bradley (1998) showed that two dissimilar Recurrence Plots (one from the Rössler system and the other from a varying-period sine wave signal) have got equal values for REC (2.1%) and have got approximately equal values for DET (42.9%, 45.8%, respectively).

3.7.4 3D surface plots of RQA

One approach to tackle some of the previously reviewed weaknesses and strengths of RP and RQA is the method of Zbilut and Webber (1992) in which 3D surface plots are created with an increase of embedding parameters (m and τ). Zbilut and Webber (1992) explored fluctuations and gradual changes in the 3D surface plots to provide information about the selection of embeddings parameters. Similarly, considering the work of Webber (2018), Marwan and Webber (2015) pointed out that the creation of

Nonlinear Analysis

3D surface plots are useful for visual selection of recurrence thresholds and embedding parameters (see Fig. 1.16 in Marwan and Webber (2015)).

With that in mind, I propose a similar graphical approach based on the works of Zbilut and Webber (1992), Webber (2018), and Marwan and Webber (2015) in order to visualise fluctuations and changes of 3D surface plots of RQA. Hence, four variables are considered to create 3D surface plots of RQA for this thesis: (i) embedding dimension, (ii) embedding delay, (iii) recurrence threshold, and (iv) metrics of RQA. Figure 3.7(A) illustrates a 3D surface plot of RQA ENTR with unitary increment of embedding parameters (m and τ) for recurrence threshold $\epsilon = 2.0$. Then, Figure 3.7(A), with other variations of recurrence thresholds (i.e., $\epsilon = 0.2$, $\epsilon = 1.0$, $\epsilon = 3.0$), is used to create Fig 3.7(B) where bands for values of τ are concatenated to form a long band that is embedded into Fig 3.7(B) (as illustrated by the arrows). Additionally, five time series with their 3D surface plots of RQA ENTR are shown in Figs 3.7(C to G) to illustrate how 3D surface plots of RQA ENTR differ from each other.

3.7 Recurrence Quantifications Analysis (RQA)

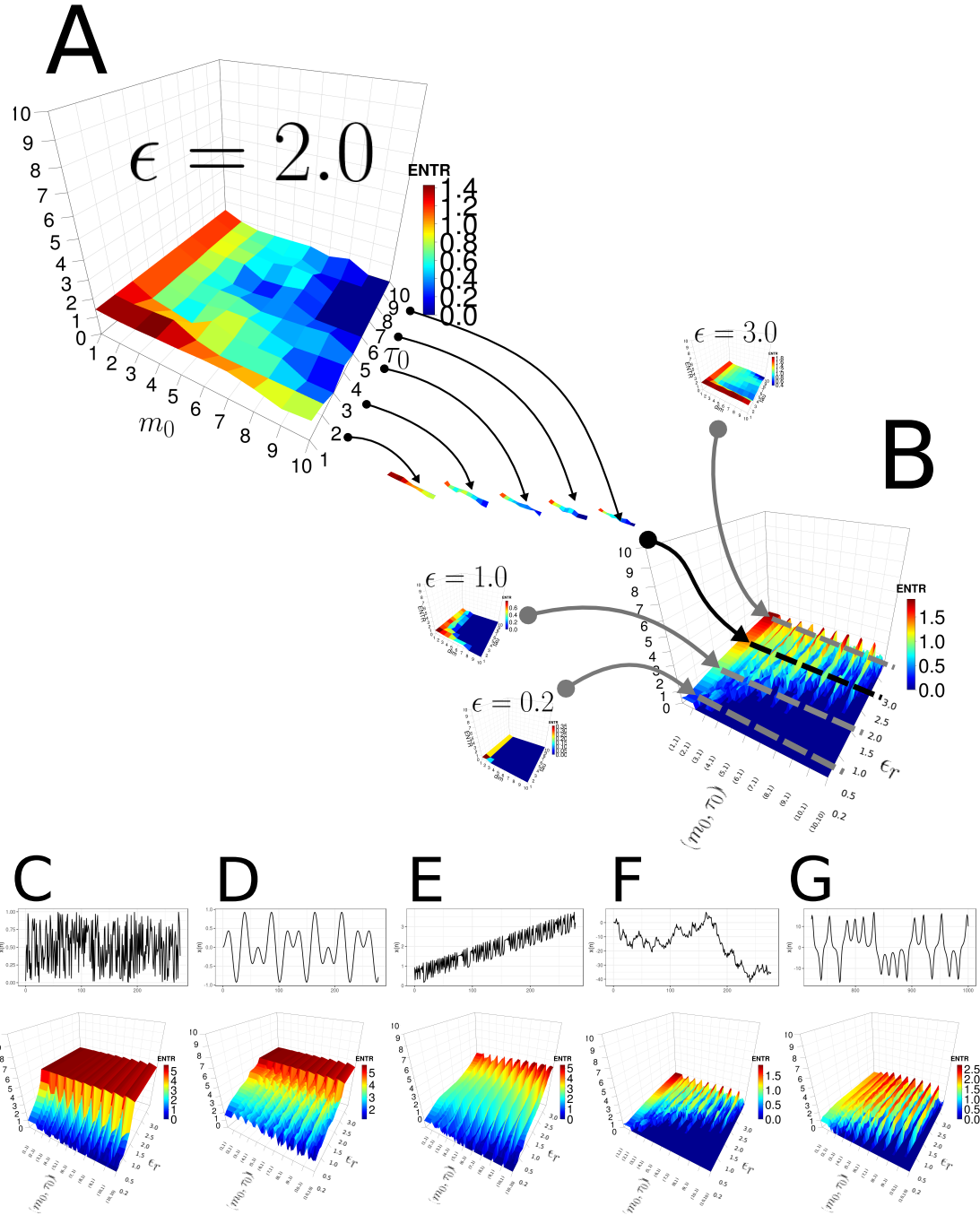


Fig. 3.7 3D surface plots. 3D surface plots of RQA ENTR incrementing (A) embedding dimensions (m and τ), (B) embedding dimensions (m and τ) and recurrence threshold (ϵ). Four time-series data and their 3D surface plots of RQA Entr for: (C) uniformly distribute noise, (D) super-positioned harmonic oscillation ($\sin \frac{1}{5}t \sin \frac{5}{100}t$), (E) drift logistic map ($x_{i+1} = 4x_i(1 - x_i)$) corrupted with a linearly increase term ($0.01i$), (F) disrupted brownian motion ($x_{i+1} = x_i + 2rnorm(1)$), and (G) $x(t)$ solution of Lorenz system. R code to reproduce the figure is available at [\[4\]](#).

3.8 Final remarks

Fundamentals of nonlinear analysis such as RSS with UTDE, estimation of embedding parameters with FNN and AMI, RP, and four RQA metrics (REC, DET, RATIO, and ENTR) were introduced in this chapter. It is important to note that this thesis is only focused on the application of traditional methods (i.e., FNN and AMI) to compute embedding parameters. See Chapter 7 for future work with optimal embedding parameters estimation. Additionally, some weaknesses and strengths of RP and RQA metrics were presented in this chapter in order to explore issues of real-world time series data. One of the contributions of this thesis is the representation of 3D surface plots of RQAs that exploit the effect of incrementing not only embedding parameters (Iwanski and Bradley, 1998) but also recurrence thresholds. See the following chapters, Chapter 4 for introduction of experiments and Chapters 5 and 6 for results.